NASA

Technical Memorandum 79588

THE EFFECT OF WIND ON THE MICROWAVE EMISSION FROM THE OCEAN'S SURFACE AT 37 GHZ

Thomas T. Wilheit

JULY 1978

National Aeronautics and
Space Administration

Goddard Space Flight Center
Greenbelt, Maryland 20771

TM 79588

THE EFFECT OF WIND ON THE MICROWAVE EMISSION FROM THE OCEAN'S SURFACE AT 37 GHZ

Thomas T. Wilheit

JULY 1978

GODDARD SPACE FLIGHT CENTER
Greenbelt, Maryland

THE EFFECT OF WIND ON THE MICROWAVE EMISSION FROM THE OCEAN'S SURFACE AT 37 GHZ

Thomas T. Wilheit

ABSTRACT

The microwave brightness temperature measurements from the Electrically Scanned Microwave Radiometer (frequency = 37 GHz) are compared with oceanic wind measurements from data buoys. It is shown that the brightness temperature can be manipulated to yield a measure of the surface roughening which can be very well accounted for by a simple geometric optics model. The data of Hollinger (1970) at 1.4, 8.36 and 19.34 GHz were similarly manipulated and shown to require a surface with less slope variance than predicted by the Cox and Monk (1955) optical measurements. It is also shown that the surface may be treated as isotropic to an accuracy equivalent to the roughening produced by a 2 m/s wind speed increment.

PRECEDING PAGE BLANK NOT FILMED

CONTENTS

THE EFFECT OF WIND ON THE MICROWAVE EMISSION FROM THE OCEAN'S SURFACE AT 37 GHZ

INTRODUCTION

There is, of course, considerable interest in measurement of the wind at the ocean surface, as it is an important input parameter to weather forecasting models and the primary input to wave forecasting models. It is further, the meteorological parameter most important to maritime and coastal operations, at least in ice-free waters. A radar experiment for the remote sensing of wind speed, the so-called Rad-Scat, was flown on the Skylab mission (Young and Moore 1977). A similar experiment, the Seasat-A Scatterometer Sensor (SASS) will be flown on Seasat-A. Both Nimbus-G and Seasat-A will carry the Scanning Multichannel Microwave Radiometer (SMMR) which, among other things, is intended to measure the wind speed at the ocean's surface. The physical principles behind this instrument have been discussed by Wilheit (1976). The relationship between microwave emissivity and wind speed has been examined experimentally from aircraft platforms by Nordberg et al (1971), Webster et al (1976) and Wilheit and Fowler (1977) and from fixed platforms by Swift (1974) and Hollinger (1970). The purpose of this paper is to examine the relationship between brightness temperature at 37 GHz as measured by the Electrically Scanned Microwave Radiometer (ESMR) aboard the Nimbus-6 Satellite and wind speed as measured by the operational data buoys operated by the National Oceanic and Atmospheric Administration (NOAA). This approach permits a wider range of conditions to be examined than would be practical in aircraft or fixed location experiments and when combined with other data provides new insight into the effect of wind on the microwave emissions of the ocean's surface.

The Electrically Scanned Microwave Radiometer (ESMR)

The Nimbus-6 satellite was launched June 12, 1975 into a sun synchronous circular orbit of 100° inclination and 1100 km altitude. The equator crossings were at approximately local solar noon (going North) and midnight (going South). The ESMR measures the thermal microwave emission in a band centered at 37 GHz (0.8 mm) in two orthogonal polarizations. The antenna beam scans along the surface of a 45° cone the axis of which is tipped approximately 5° forward of the local vertical. The scan procedes from 25° to the right in front of the spacecraft to 25° to the left in 72 discrete beam positions every 5-1/3 seconds. The incidence angle of the antenna beam is approximately constant at 50° throughout the scan. The instrument design and operating principles have been discussed more thoroughly by Wilheit (1975).

Observations

Power constraints only permitted the instrument to be operated approximately 50% of the time during the first year after launch (June 1975-June 1976). After June of 1976, failures and depletions of other experiments permitted essentially full-time operation of the ESMR until mid-September 1976 when the horizontally polarized channel failed. Thus, half-time data were collected for one year and full-time data were collected for three months.

Examination of the data revealed two problems affecting calibration, apparent modulation of the loss of the antenna during the orbit and excess noise when measuring the radiation from the warm calibration load. The modulation of the antenna loss was found to be consistent with respect to sun angle. It showed its maximum rate of change as the spacecraft entered the sunlight with the instrument facing the sun and fairly rapid changes whenever the spacecraft was in the sunlight. The

changes were rather gradual whenever the spacecraft was in darkness. The most reasonable explanation seems to be thermo-mechanical warping of the radome modulating the coupling among the radiating elements in the antenna. No cause is easily discerned for the excess noise on the warm calibration load. An empirically derived correction has been applied to the data to mitigate the effects of these problems. It was found that the residual error of these problems was excessive for this study whenever the instrument was in the sun. We have, therefore, used only nighttime data.

The direct measurements of wind speed used in this report were made by the operational data buoys operated by NOAA. The buoys used in this study, their (old) EB designations, their (new) station identifications, their locations and the height at which they measure the wind speed are given in Table 1. The buoys report wind speed and direction, air temperature sea surface temperature, surface pressure, dew point and other meteorological and oceanographic parameters generally at three hour intervals.

At any one time during the period of this experiment approximately three quarters of the buoys listed would be operating and reporting. The data were obtained from the National Climatic Data Center (NOAA), Asheville, NC; one tape covered the entire data set from 1972 through April 1977 (the time at which the tape was ordered).

It is necessary in analyzing these data to remove the effect of varying measurement height and atmospheric stability (air-sea temperature difference). To this end a boundary layer wind shear model provided and discussed by V. Cardone (1969) was used. This model was used to calculate the wind friction velocity, generally termed U* ("U-Star") from the measured wind speed, air temperature

and sea temperature. It is this surface friction velocity which is, presumably, correlated with the microwave emissivity of the surface. However, in order to convert this to a more familiar parameter, this surface stress was converted to a wind speed at 20 meters altitude assuming neutral stability (sea temperature equal to air temperature). In this study, this so derived 20 meter wind will be termed "neutral stability wind speed." It must be emphasized that the conversion from surface stress to equivalent wind speed is simply a change of scale (albeit somewhat nonlinear) and is done for the convenience of dealing in familiar quantities.

The data set for this experiment was generated by first searching all the appropriately calibrated data tapes from Nimbus-6 ESMR for observations within 50 km of the nominal locations of each of the data buoys. All observations for which the horizontally polarized brightness temperature exceeded 220°K were rejected as this would indicate a large atmospheric opacity. The remainder were averaged in each polarization for each data buoy and orbit and those averages containing at least nine samples were retained. Those with fewer than nine either had excessive atmospheric opacity or were too near the edge of the ESMR swath to get enough samples. These samples were then compared with the buoy data to pair radiometer and wind observations. The wind speeds and directions are linearly interpolated in time between the buoy interrogations proceeding and following the radiometer data to the time of the radiometer sample. If the wind speed changes by more than 2.5 m/s (or 20% whichever is larger) between the two samples the pair is rejected. Also if the time interval between the samples is greater than 3 hours the pair is rejected. Even with these conditions, 264 data pairs were collected, distributed as indicated in Table I. With each data pair, the raw wind

speed and direction were saved and, using the air and sea temperature provided by the buoys, the neutral stability wind speed and the true 20 meter wind speeds were also calculated and retained.

Theoretical Model

For sake of relating the brightness temperature measured by the Nimbus-6 ESMR to the wind speed we will develop an approximate theory. The viewing geometry is as shown in Figure 1. We have approximated the atmosphere as a single layer with a transmissivity $A(\theta)$ at an angle θ and a temperature T_1, the surface has a temperature T_2, a reflectivity R_i and is assumed to be a specular reflector. The subscript i refers to the polarization and can be either H (for horizontal polarization) or V (for vertical polarization). To calculate the observed upwelling brightness temperature one begins with T_{CB}, the 2.7°K cosmic background. At the base of the atmosphere the downwelling brightness is then

$$T_B = A(\theta)T_{CB} + (1 - A(\theta))T_1$$

After reflection from the surface, the upwelling brightness becomes

$$T_{Bi} = R_i(\theta)(A(\theta)\, T_{CB} + (1 - A(\theta))T_1) + (1 - R_i(\theta))\, T_2$$

and finally at the top of the atmosphere

$$T_{Bi} = R_i(\theta)(A^2(\theta)\, T_{CB} - (A(\theta) - A^2(\theta))T_1)$$

$$+ A(\theta)(1 - R_i(\theta))\, T_2 + (1 - A(\theta))\, T_1$$

If we make the approximation

$$T_1 \approx T_2$$

then

$$T_{Bi} = (1 - R_i(\theta)\, A^2(\theta))\, T_1 + R_i(\theta)\, A^2(\theta)\, T_{CB}$$

and it follows that

$$\frac{T_{BH} - T_1}{T_{BV} - T_1} = \frac{R_H(\theta)}{R_V(\theta)}$$

Since it has been shown that the microwave reflectivity of the ocean surface is in general a function of wind speed, then the ratio of reflectivity is also a function of wind speed unless the dependence fortuitously cancels. Therefore, we define

$$F_{T_1}(W) = (T_1 - T_{BH})/(T_1 - T_{BV})$$

The purpose of this paper is to examine the wind speed, W, dependence of $F_{T1}(W)$.

In principle, $F_{T1}(W)$ is also a function of the sea surface temperature and salinity. At the frequency of interest here, 37 GHz. The salinity dependence is quite inconsequential; the temperature dependence will be examined in an appendix.

It is enlightening if, for the moment, we consider the effect of wind speed on the surface reflectivity to be through the two mechanisms of roughness and partial coverage of the surface with a nonreflective substance (foam). We can then express the surface reflectivity $R_i(\theta, W) = f(W)R'(\theta, W)$ where f(W) is the fraction of the surface covered by foam and R' is the reflectivity of the remainder of the surface. It then follows that:

$$F_{T_1}(W) = R'_H(\theta, W)/R'_V(\theta, W)$$

That is, the same manipulation which eliminates the atmospheric opacity from the problem also eliminates foam to the extent that foam can be described as a non-reflective surface and we are left with a measure of the roughening of the surface.

To continue with this concept we may also approximate the effect of roughening the surface by treating the surface as an isotropic ensemble of a flat facets with various inclinations as viewed by the radiometer as described by Cox and Monk (1965) and calculate the reflectivity of each facet by use of the Fresnel relations (Jackson 1962) and the Lane and Saxton (1953) dielectric data. Those rays which are reflected at a sufficiently low angle to have to undergo a second surface reflection are assumed to be totally absorbed. This is substantially a conventional geometric optics model.

The results of this model are compared with measurements in the resulting section.

The temperature to be assigned to the surface and the atmosphere, T_1 is still unspecified. One would reasonably expect that a value in the 285-290°K range would be appropriate. Since we are dealing with brightness temperatures much lower than this, little sensitivity to the exact value would be expected; this point will be examined in the results section.

Results

First the data were examined to determine the appropriate value of T_1. The correlation coefficient between the ratio

$$F_{T_1} = \frac{T_{BH} - T_1}{T_{BV} - T_1}$$

and the wind speed (defined three different ways) was examined as a function of T_1. The results are shown in Figure 2. The correlation coefficients for all three wind definitions show a broad maximum in the 285-290°K range confirming the expectation that T_1 should have a value typical of the Earth's surface

and that the results should be fairly insensitive to its precise value. Henceforth, we will use the value $T_1 = 285°K$. It is also interesting to note that the neutral stability wind speed shows the highest correlation coefficient although the degree of improvement over the raw wind speed (actual measurements at 5 or 10 meters height) is not great.

The calculated actual wind at 20m altitude yields much worse results. Though hardly conclusive, the results certainly suggest that the neutral stability wind speed is a reasonable quantity to be compared with microwave radiometric measurements.

To examine the relationship between F_{285} and the neutral stability wind speed, the data were grouped in intervals of 3kt(1.5 m/s). The results are given in Table II and in Figure 3. The data are reasonably well fit by the line: $F_{285} = 1.85 - .0132W$ where the wind speed W is in meters/second. The RMS scatter of the individual points about this line is .062 which corresponds to 4.7 m/s. This is easily accounted for by an error budget which includes both instrument noise and spacecraft pitch uncertainty but is dominated by a residual relative calibration uncertainty of 2°K in both polarizations. The assumed standard error for the averaged observations is $.0062/\sqrt{n}$, where n is the number of observations in the average.

The comparison in Figure 3, between the data and the geometric optics model described in the theoretical model section is quite striking. None of the points differ from the model calculation by more than about twice their standard error. These results suggest that the geometric optics model based on a Cox and Monk (1955) surface gives a very good description of a wind roughened ocean surface at 37 GHz at least near 50° incident angle.

The data of Hollinger (1970) are in a form that makes them comparable. In particular, he gives the brightness temperature as a function of wind speed for both polarizations at 55° incidence angle for an ocean temperature of 291°K. In analyzing the data, he has applied a rather arbitrary filter which should remove most of the foam effect; by using the ratio technique discussed here the remainder of the foam effect as well as atmospheric effects can be removed.

In Table II the value of the slope of $F_{291}(W)$ are given for the Hollinger (1970) data for the three frequencies at which he made measurements. In all three cases the geometric optics overestimates the slope. This may be interpreted by assuming that only part of the roughness spectrum which provided the slope variance optically measured by Cox and Monk (1954) is effective at these longer wavelengths (1.5-21 cm) but that 37 GHz (0.8 cm) the entire roughness spectrum is observed. The fractions required to rectify the model to the observations are given in Table II and in Figure 4. The Hollinger (1970) results show an increase in this fraction that is nearly linear in frequency and suggest a saturation at the full Cox and Monk (1955) slope variance at about 35 GHz presumably remaining at that value all the way to optical frequencies. Extrapolating this trend to lower frequencies does not go to zero variance but, of course, such an extrapolation across the entire gravity wave spectrum would be difficult to support.

Since we have also retained wind direction data, we may examine the effect of the relationship between the direction of the wind and viewing geometry. In all these data the view heading is 195° ± 30°, i.e., generally a little to the west of south. In Figure 5, the residual, $F_{285} + .0132W$, is plotted versus wind direction averaged in 20° intervals. There is no believable pattern visible. The data

were also grouped in 20 degree intervals with respect to the view direction. These data are shown in Figure 6. The first five points have been plotted twice to continue the data across 360°. They also are consistent with no wind direction effect. Any effect larger than about 0.02 would be detectable here suggesting that if there is a wind direction effect it corresponds to less than about 2 m/s in wind speed. Thus the use of the isotropic Cox and Munk data seem justified.

SUMMARY

By comparing data from the Nimbus-6 ESMR with wind speeds measured by operational data buoys and by examining the data of Hollinger we have shown that the effect on microwave emissivity of wind roughening of the sea surface may be accounted for with a simple geometric optics model wherein the slope variance is given by a portion of the Cox and Munk (1955) isotropic distribution as shown in Figure 4. It is also suggested that microwave observations of the ocean surface may be more nearly related to the friction velocity than to the actual wind speed measured at any arbitrary height.

ACKNOWLEDGMENT

The author gratefully acknowledges the assistance of the very helpful personnel of the National Data Buoy Office and the National Climatic Data Center.

REFERENCES

1. Cardone, V. J., "Specification of the Wind Distribution in the Marine Boundary Layer for Wave Forecasting," Ph.D Thesis, New York University, Department of Meteorology and Oceanography, 1969 (Available from NTIS Order #AD702490).
2. Cox, C. and Munk, W., "Some Problems in Optical Oceanography," J. Marine Res. 14, 63-78 (1955).
3. Hollinger, J. P., "Passive Microwave Measurements of Sea Surface Roughness," Trans. IEEE Geoscience Electronics, GE-9, pp 165-169 (1971).
4. Jackson, J. D., "Classical Electrodynamics," John Wiley & Sons, Inc., New York (1962), p 216ff.
5. Lane, J. A. and J. A. Saxton, "Dielectric Dispersion in Pure Polar Liquids at Very High Radio Frequencies," Proc. Roy. Soc., London A, 214, pp 531-545, (1952).
6. Nordberg, W., J. Conaway, D. B. Ross, and T. Wilheit, "Measurements of Microwave Emission from a Foam-Covered Wind Driven Sea," J. Atmos. Sci., 38, 429-435, (1971).
7. Swift, C. T., "Microwave Radiometer Measurements of the Cape Cod Canal," Radio Science 9, 641-653, (1974).
8. Webster, W. J., Jr., T. T. Wilheit, D. B. Ross, and P. Gloersen, "Spectral Characteristics of the Microwave Emission from a Wind Driven Foam-Covered Sea," J. Geophys. Res. 81, 3095-3099 (1976).
9. Wilheit, T., "The Electrically Scanning Microwave Radiometer (ESMR) Experiment," Nimbus-6 User's Guide, NASA/Goddard Space Flight Center, Greenbelt, Maryland 87-108 (1975).

10. Wilheit, T. T., "A Review of Applications of Microwave Radiometry to Oceanography," NASA X-953-77-27 (1977) also: to be published in Boundary Layer Meteorology.

11. Wilheit, T. T., M. G. Fowler, "Microwave Radiometric Determination of Wind Speed at the Surface of the Ocean During BESEX," Joint Issue Trans. IEEE Ant. and Prop 25 111-120 (1977), and Trans. IEEE Oceanic Eng. 2 111-120 (1977).

APPENDIX

SEA SURFACE TEMPERATURE DEPENDENCE

The measurements of the dielectric properties of saline solutions by Lane and Saxton (1952) reveal a strong temperature dependence and a modest salinity dependence except at low frequencies (~ 5 GHz) where the saline conductivity becomes important. Thus the reflectivities calculated from these dielectric properties will also be a function of temperature. Specifically if the reflectivity ratio ($F(W) = R_H/R_V$ for 50° incidence angle and 37 GHz is calculated for a smooth surface as a function of temperature it is found that it varies from a value of 1.89 to 1.72 over the 278-303°K range of our measurements. However, our measurements are not of the reflectivity ratios themselves but rather the brightness temperatures. Thus we have calculated value of

$$F_{T_1}(W) = (T_1 - T_{BH})/(T_1 - T_{BV})$$

for a value of $T_1 = 285°K$ and for several frequency choices. The results are shown in Figure A-1 for a range of frequencies. It can be seen here that for the range of sea surface temperature encountered the net variation is only about ±.01, which would reduce the correlation coefficient between wind speed and F by only about 2%. This is merely a fortuitous result of the frequency choice. Other choices of T_1 give similar results, thus this is not the cause of the best correlations occurring at $T_1 = 285$.

Table I

EB #	Station ID	Wind Height Meters	Latitude (North)	Longitude (West)	Data Pairs
1	41001	10	35.0	72.0	5
3	46001	10	56.0	148.0	25
4	42001	10	26.0	90.0	29
15(13)	41002	10	32.3	75.3	39
16	46002	10	42.5	130.0	52
17	46003	10	52.0	156.0	18
19	46004	10	51.0	136.0	10
34	44002	5	40.1	73.0	33
35	–	5	55.3	157.0	5
41	44001	5	38.7	73.6	40
61	–	10	28.5	90.9	6
70	–	10	59.5	142.2	2
				Total	264

Table II

Wind Speed Interval (m/s)	Number of Samples	Average F_{285}	Standard Error in Average
0-1.5	10	1.82	.0020
1.5-3.0	18	1.82	.0015
3.0-4.5	30	1.80	.0011
4.5-6.0	40	1.77	.0010
6.0-7.5	52	1.75	.0009
7.5-9.0	43	1.74	.0009
9.0-10.5	25	1.73	.0012
10.5-12.0	22	1.69	.0013
12.0-13.5	13	1.72	.0017
13.5-15.0	3	1.62	.0036
15.0-16.5	3	1.75	.0036
16.5-18.0	3	1.64	.0036
21	1	1.65	.0062
34	1	0.32	.0062

Table III

Comparison of Hollinger (1970)
with Geometric Optics
F_{291} = A - BW; $\theta \simeq 55°$

Frequency GHz	B Observed	Required Fraction of Cox and Monk Variance
1.4	.0020 S/M	.33
8.36	.0041 S/M	.44
19.34	.0093 S/M	.75

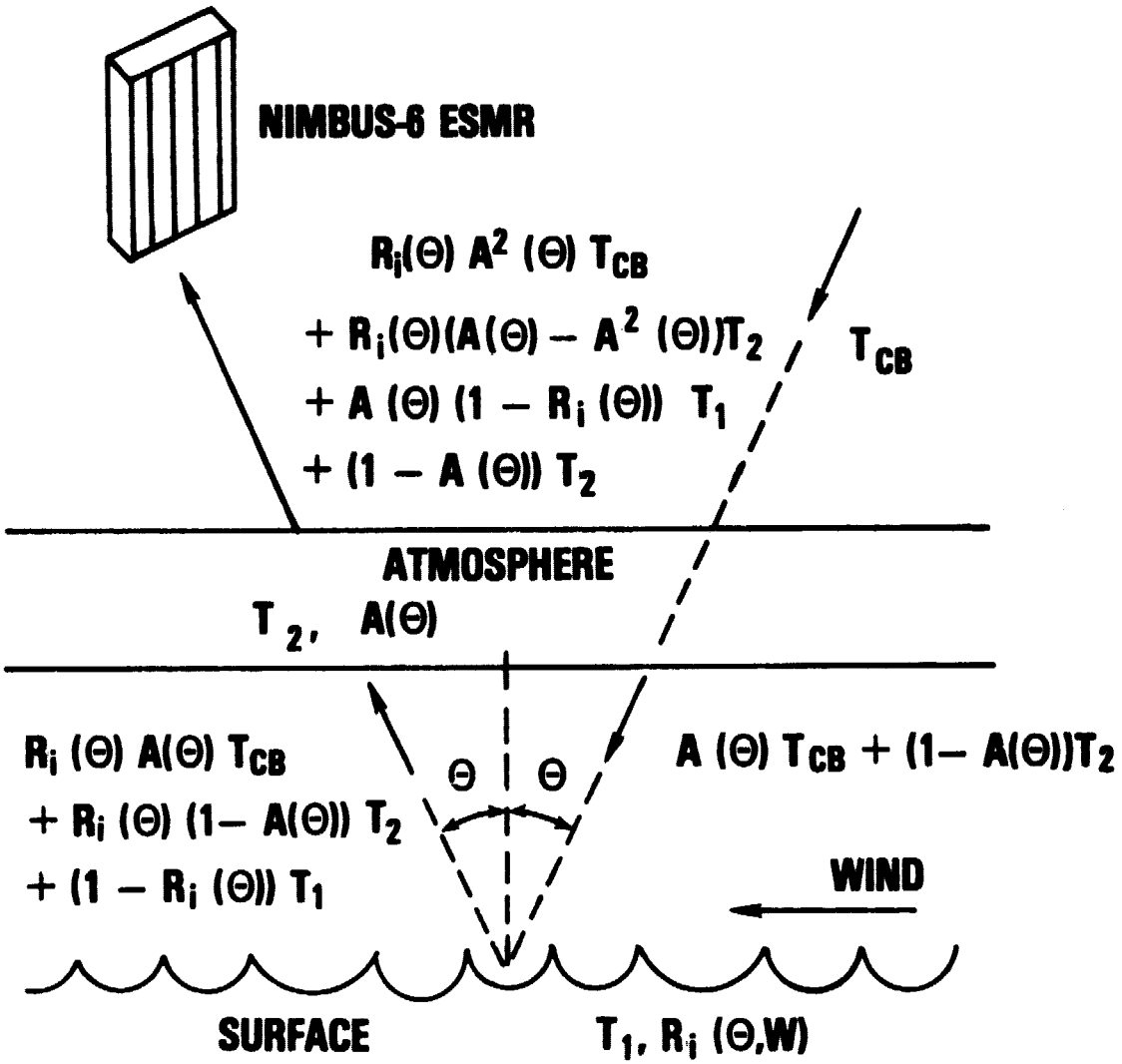

Figure 1. Viewing geometry for simplified radiation transfer model with relevant brightness temperature indicated

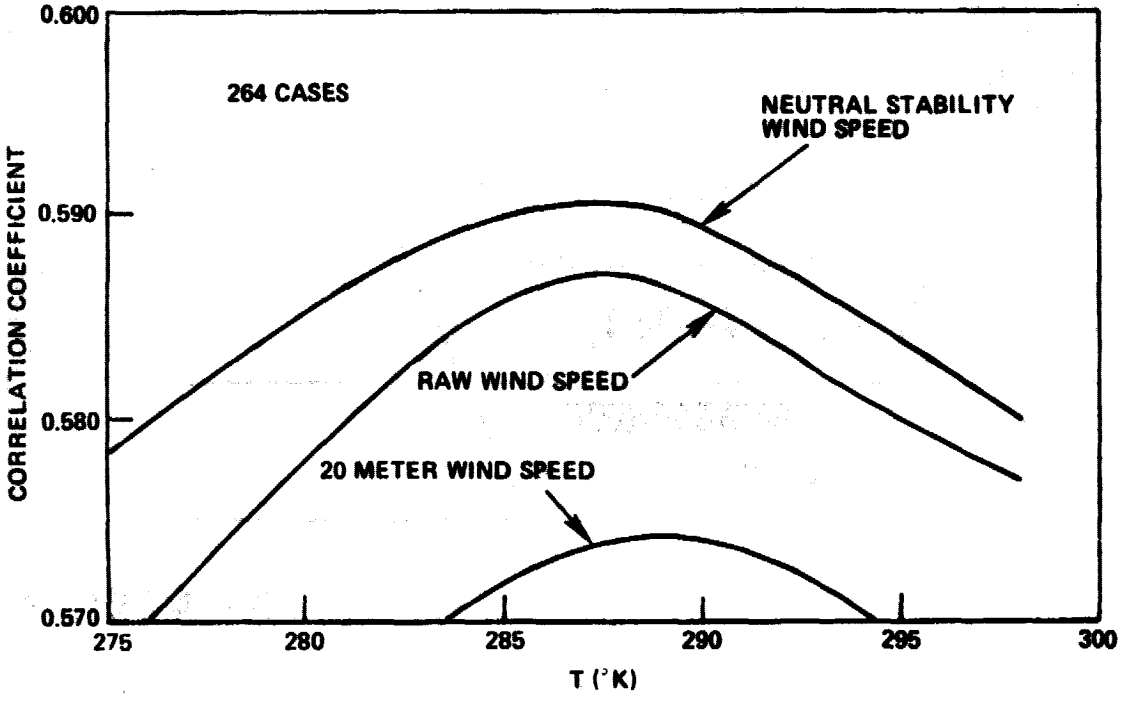

Figure 2. Correlation coefficient between F_{T_1} and wind speed as a function of T_1 for three different wind speed measures

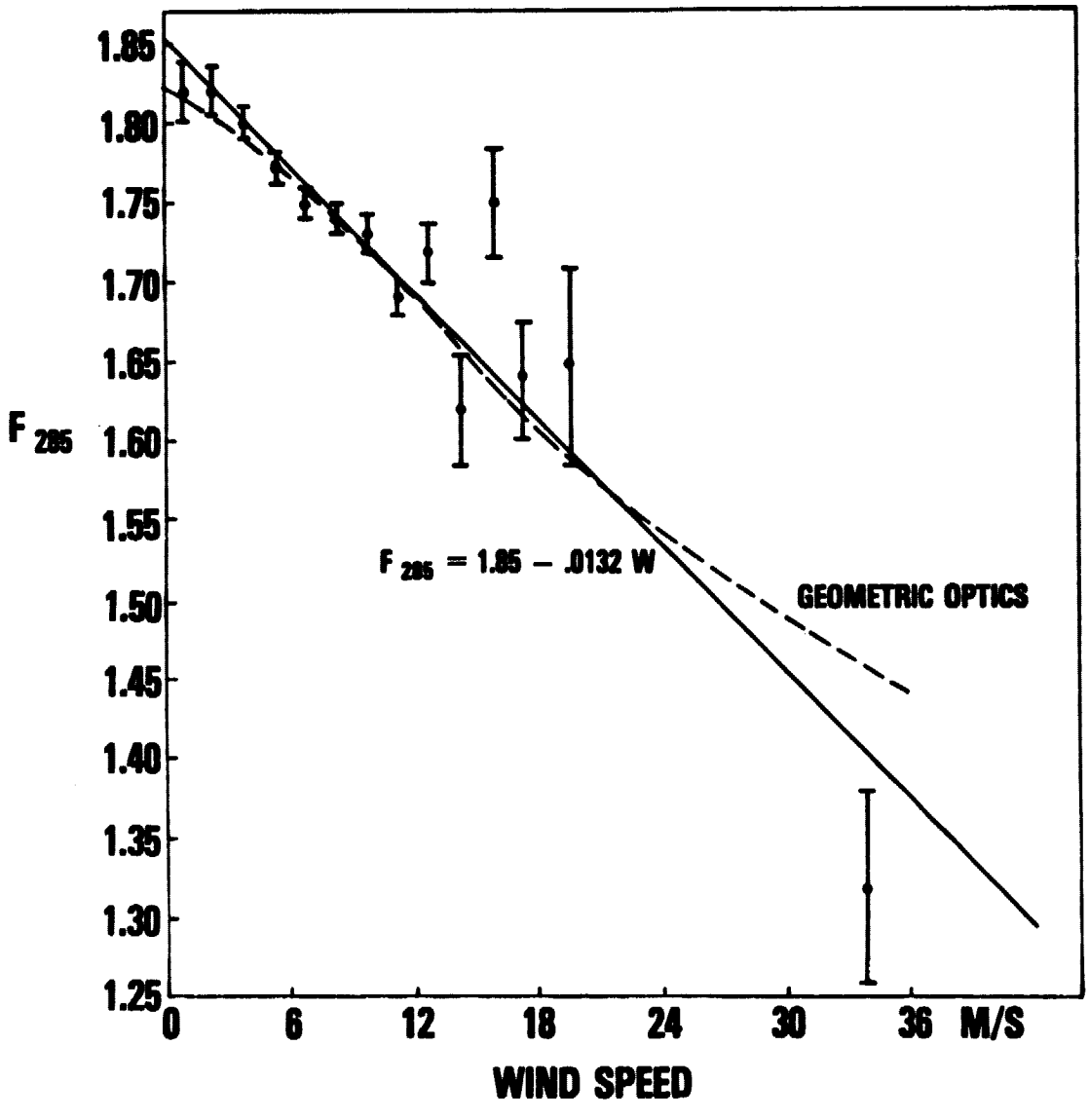

Figure 3. Comparison between observed values of F_{285} and wind speed averaged over 1.5 m/s intervals

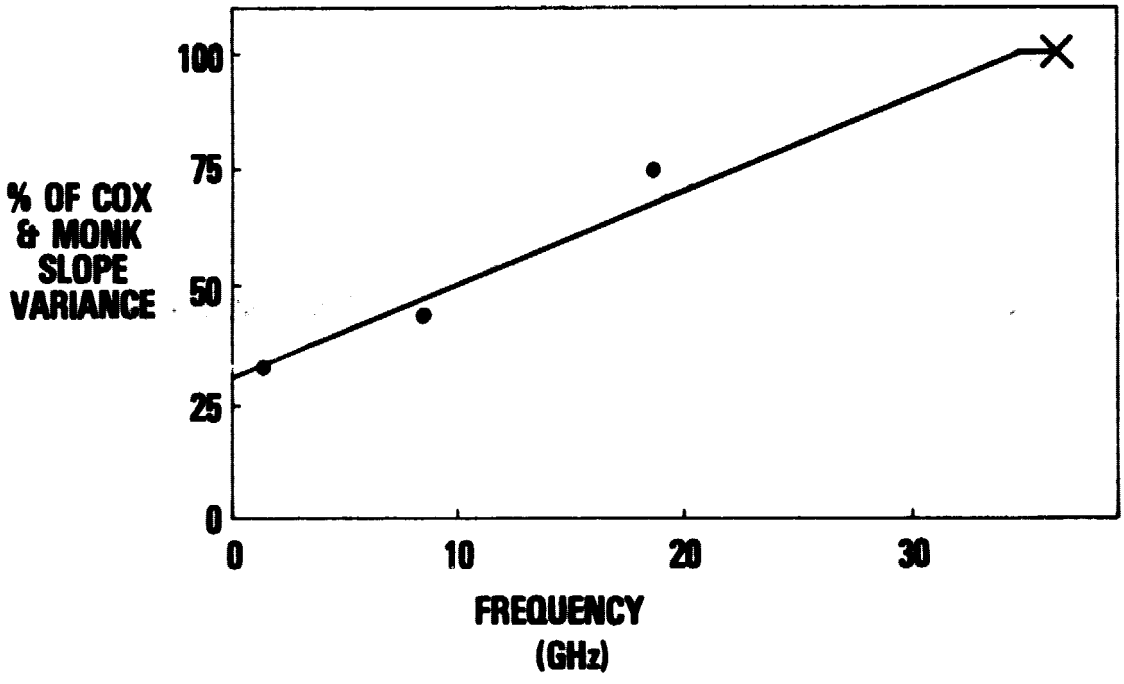

Figure 4. Percentage of Cox and Monk (1955) slope variance required for a geometric optics model to explain the observations of this paper (X) and Hollinger (1971) (•) as a function of frequency

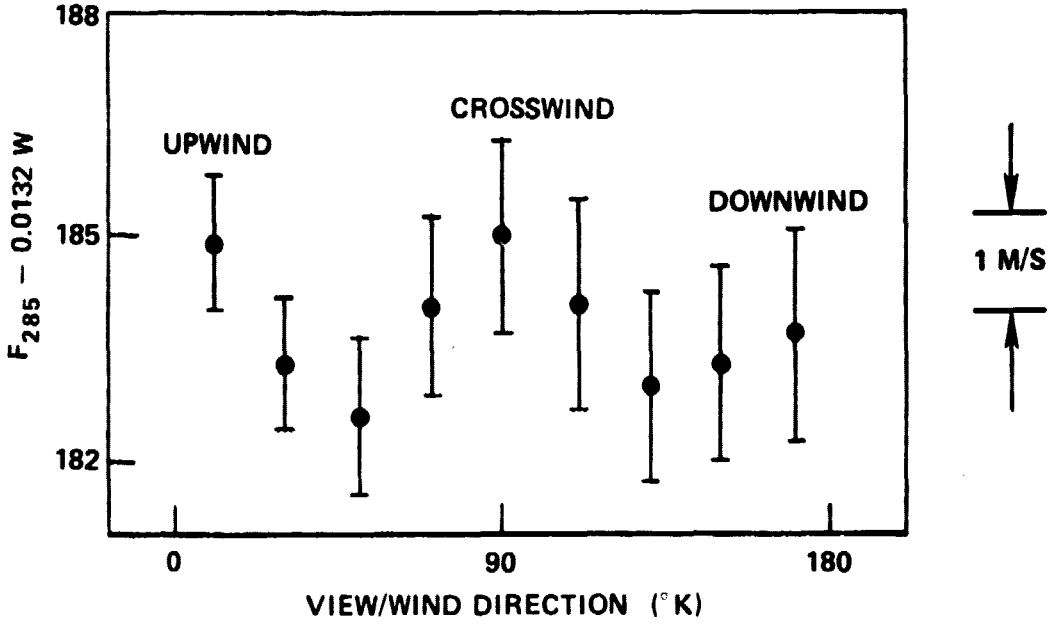

Figure 5. Residual of F_{285} with wind speed effect removed as a function of relative angle between viewing direction and wind direction

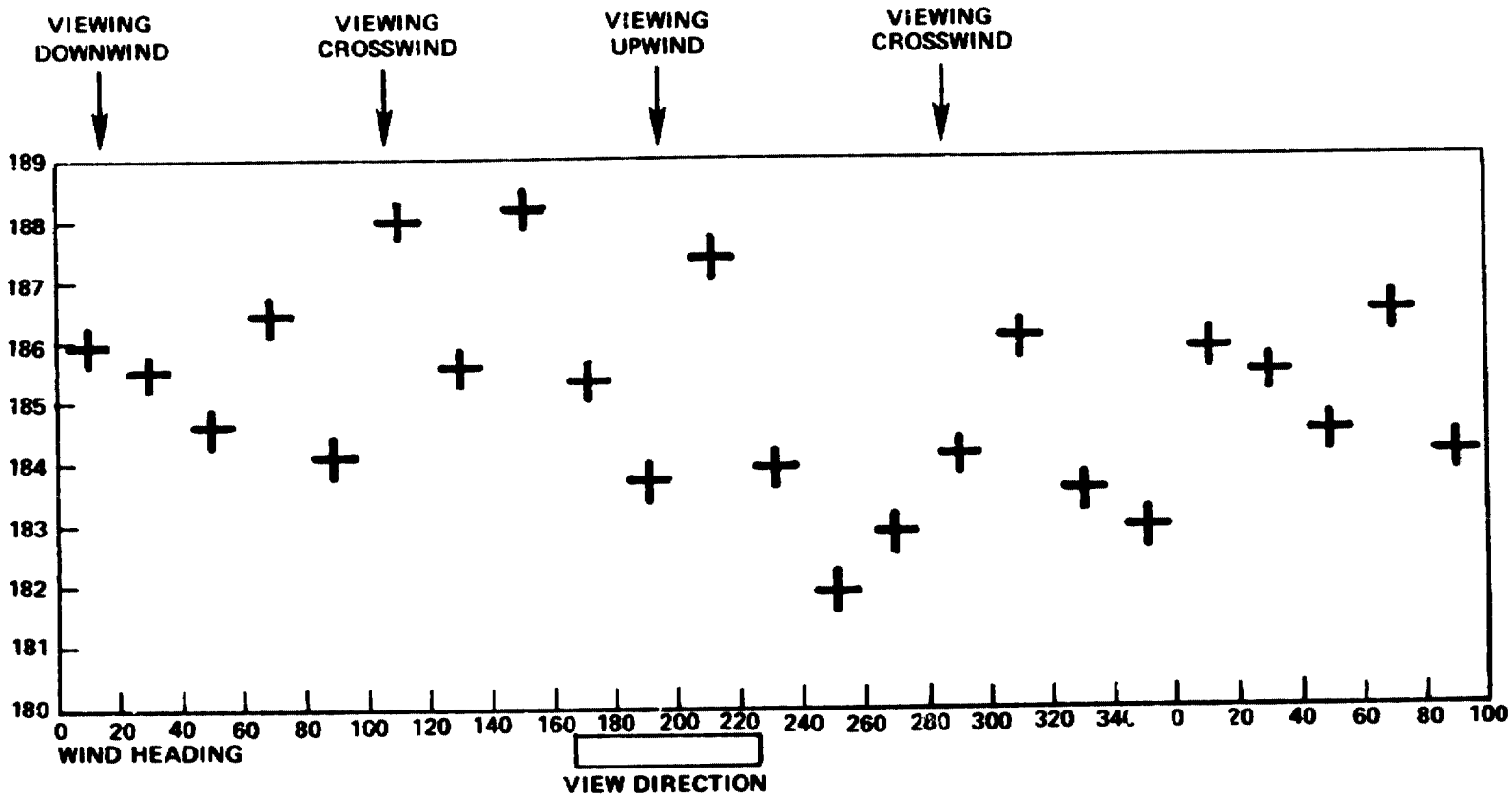

Figure 6. Residual of F_{285} with wind speed effect removed as a function of absolute wind heading

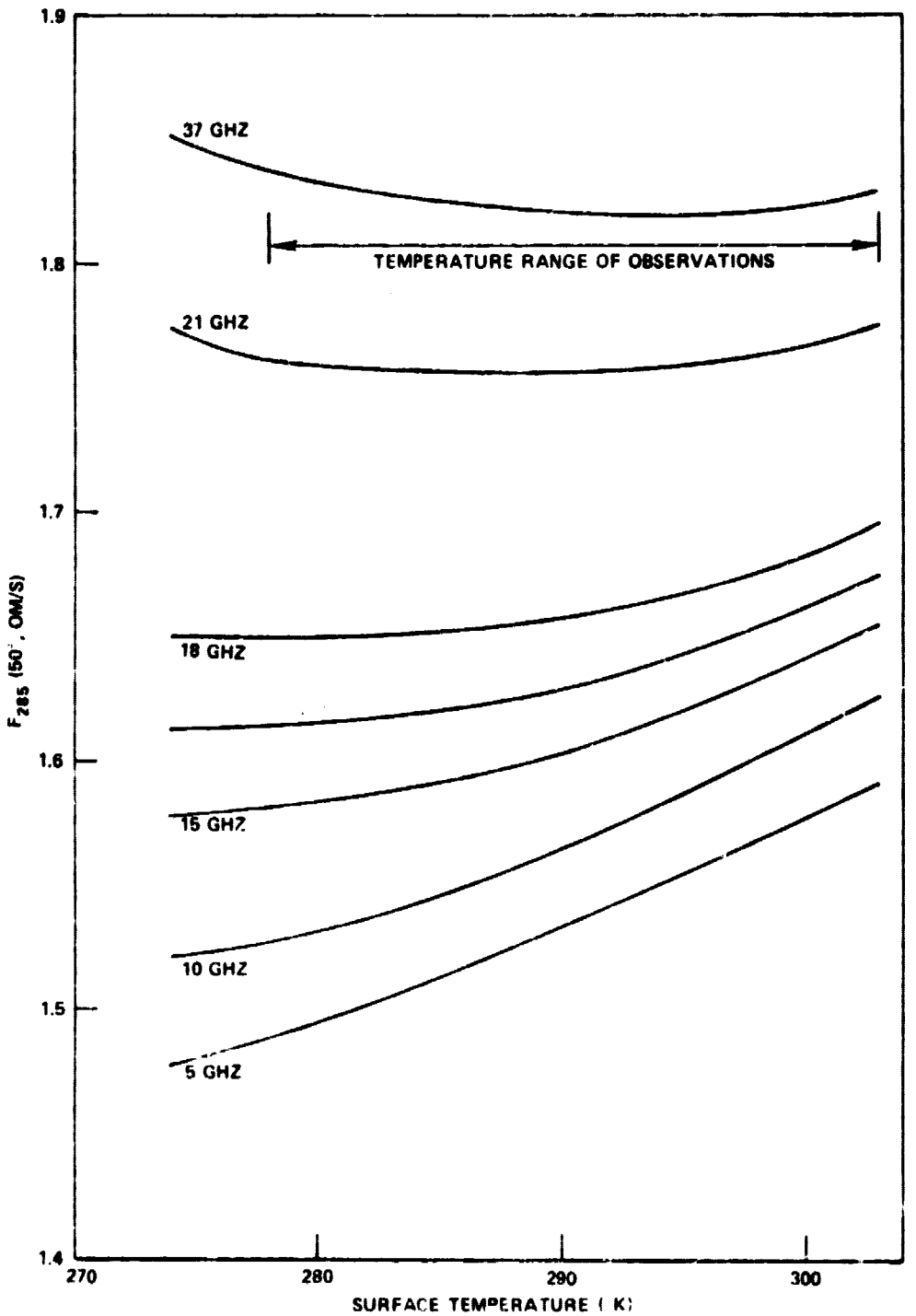

Figure A-1. F_{285} or a function of surface temperature for several frequencies

Figure Captions

Figure 1. Viewing geometry for simplified Radiation Transfer Model with relevant brightness temperatures indicated

Figure 2. Correlation coefficient between F_{T_1} and wind speed as a function of T_1 for three different wind speed measures

Figure 3. Comparison between observed values of F_{285} and wind speed averaged over 1.5 m/s intervals

Figure 4. Percentage of Cox and Monk (1955) slope variance required for a geometric optics model to explain the observations of this paper (X) and Hollinger (1971) (•) as a function of frequency

Figure 5. Residual of F_{285} with wind speed effect removed as a function of relative angle between viewing direction and wind direction

Figure 6. Residual of F_{285} with wind speed effect removed as a function of absolute wind heading.

Figure A-1. F_{285} or a function of surface temperature for several frequencies